



Available online at www.sciencedirect.com

ScienceDirect

European Journal of Protistology 50 (2014) 593–605

European Journal of
PROTISTOLOGY

www.elsevier.com/locate/ejop

Morphology and phylogenetic position of the oxytrichid ciliates, *Urosoma salmastra* (Dragesco and Dragesco-Kernéis, 1986) Berger, 1999 and *U. karinae sinense* nov. ssp. (Ciliophora, Hypotrichia)

Chen Shao^{a,*}, Lingyun Chen^{a,b}, Ying Pan^b, Alan Warren^c, Miao Miao^d

^aThe Key Laboratory of Biomedical Information Engineering, Ministry of Education, School of Life Science and Technology, Xi'an Jiaotong University, Xi'an 710049, China

^bLaboratory of Protozoology, Institute of Evolution and Marine Biodiversity, Ocean University of China, Qingdao 266003, China

^cDepartment of Life Sciences, Natural History Museum, London SW7 5BD, UK

^dCollege of Life Sciences, University of Chinese Academy of Sciences, Beijing 100049, China

Received 1 January 2014; received in revised form 10 August 2014; accepted 11 August 2014
Available online 27 August 2014

Abstract

The morphology and infraciliature of two hypotrichous ciliates, *Urosoma salmastra* and *U. karinae sinense* nov. ssp., were investigated for populations collected from the surface of intertidal gravel in the Huguang Mangrove Forest, Zhanjiang, China and the upper 10 cm layer of soil in the Sangke Grass Land in the southern part of Gansu Province, China, respectively. *Urosoma salmastra* is characterized by its elongate-elliptical body with no tail-like structure; two macronuclear nodules; cortical granules colourless, less than 1 μm across, and arranged in short rows; adoral zone occupying 25% of body length in vivo; paroral conspicuously short and located in front of endoral. *Urosoma karinae sinense* nov. ssp. is characterized by its elongate-elliptical body with no tail; 2–4 macronuclear nodules; cortical granules colourless, less than 1 μm across, and arranged in short rows; adoral zone occupying 30% of body length in vivo; paroral shorter than, and located ahead of endoral. Phylogenetic analyses based on SSU rRNA gene sequence data suggest a close relationship between *U. salmastra*, *U. karinae sinense* nov. ssp. and *Oxytricha granulifera* within the Oxytrichinae assemblage.

© 2014 Elsevier GmbH. All rights reserved.

Keywords: Hypotrichia; Morphology; Oxytrichidae; *U. karinae sinense*; *Urosoma salmastra*

Introduction

Oxytrichidae is one of the largest families in the subclass Hypotrichia and was comprehensively reviewed by Berger

(1999) who recognized 169 valid species. In recent years several new genera and species have been reported and the *Gonostomum*-like forms (oral apparatus and dorsal ciliature both in *Gonostomum*-pattern) have been removed from this family (Berger 2011; Chen et al. 2013a,b; Gupta et al. 2006; Küppers et al. 2011; Li et al. 2010, 2013; Lv et al. 2013; Shao et al. 2011, 2013a,b; Shi et al. 2002; Singh and Kamra 2013; Singh et al. 2013; Song 1990, 2001; Song and Warren 1999; Song and Wilbert 1997a,b, 2002; Weisse et al. 2013).

*Corresponding author. Tel.: +86 29 8266 8463.

E-mail addresses: shaochen@xjtu.edu.cn, andrews1201@hotmail.com (C. Shao).

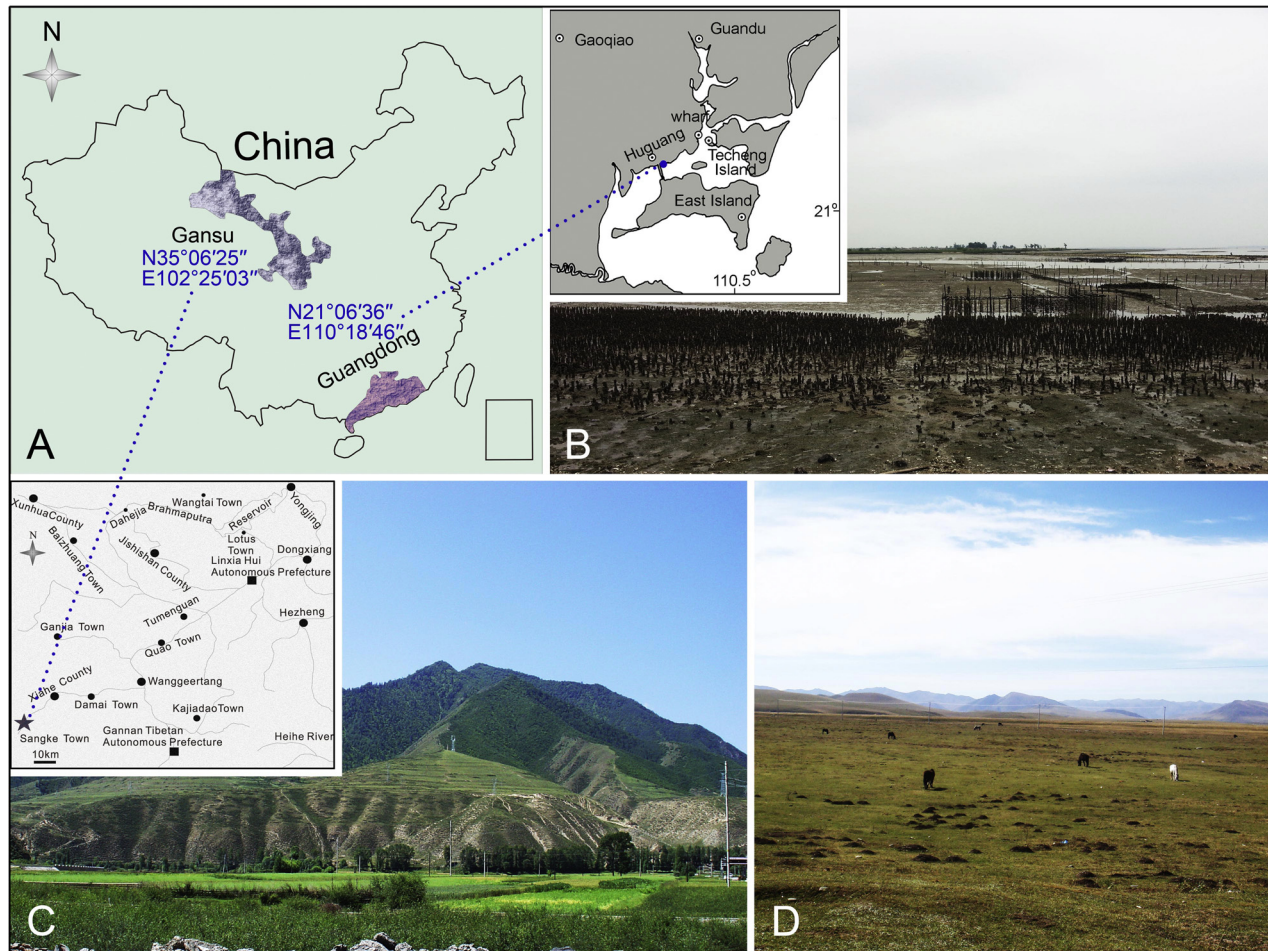


Fig. 1. The sample sites and surrounding areas. (A) Map and insets showing the locations of Huguang Mangrove Forest, Zhanjiang, China and Sangke Grass Land, Gansu Province, China. (B) Showing the location at the Huguang Mangrove Forest where the sample containing *Urosoma salmastra* was collected. (C, D) Showing the location at the Sangke Grass Land where the sample containing *U. karinae sinense* nov. ssp. was collected.

The oxytrichid genus *Urosoma* Kowalewskiego, 1882 is characterized by its adoral zone of membranelles and undulating membranes in a *Gonostomum*-pattern, cirrus III/2 displaced anteriorly, dorsal ciliature in *Urosomoida*-pattern, and the presence of caudal cirri (Berger 1999). Ten species have been assigned to *Urosoma*, nine of which have been investigated using both live observations and protargol preparations, the exception being *U. salmastra* which is known only from silver-stained specimens (Dragesco and Dragesco-Kernéis 1986) and was considered by Berger (1999) as possibly synonymous with *U. karinae*.

In November 2010 and October 2011, two populations of oxytrichid ciliates were isolated from the surface of intertidal gravel in the Huguang mangrove forest, Zhanjiang, southern China and the upper 10 cm layer of soil in the Sangke Grass Land, Gansu Province, China. They were identified as *U. salmastra* and *U. karinae sinense* nov. ssp. In the present study, we reported the morphology of these two taxa from live observations and protargol preparations and used these data

to distinguish *U. salmastra* from *U. karinae*. In addition the phylogenetic placement of the two species was determined, using sequences of the gene coding for small subunit (SSU) rRNA.

Material and Methods

Sampling and cultivation (Fig. 1A–D)

Urosoma salmastra was collected from the surface of intertidal gravel in the Huguang Mangrove Forest, Zhanjiang (21°06' N; 110°18' E), Guangdong Province, China on 25 November 2010 when the water temperature was 24 °C, pH 7.3, and salinity 25.5‰ (Fig. 1A, B). *Urosoma karinae sinense* nov. ssp. was collected from the upper 10 cm layer of soil in the Sangke Grass Land (35°06' N; 102°25' E), Gansu Province, China on 24 October 2011 when the soil temperature was 7 °C, pH 8.0, and air temperature 16 °C

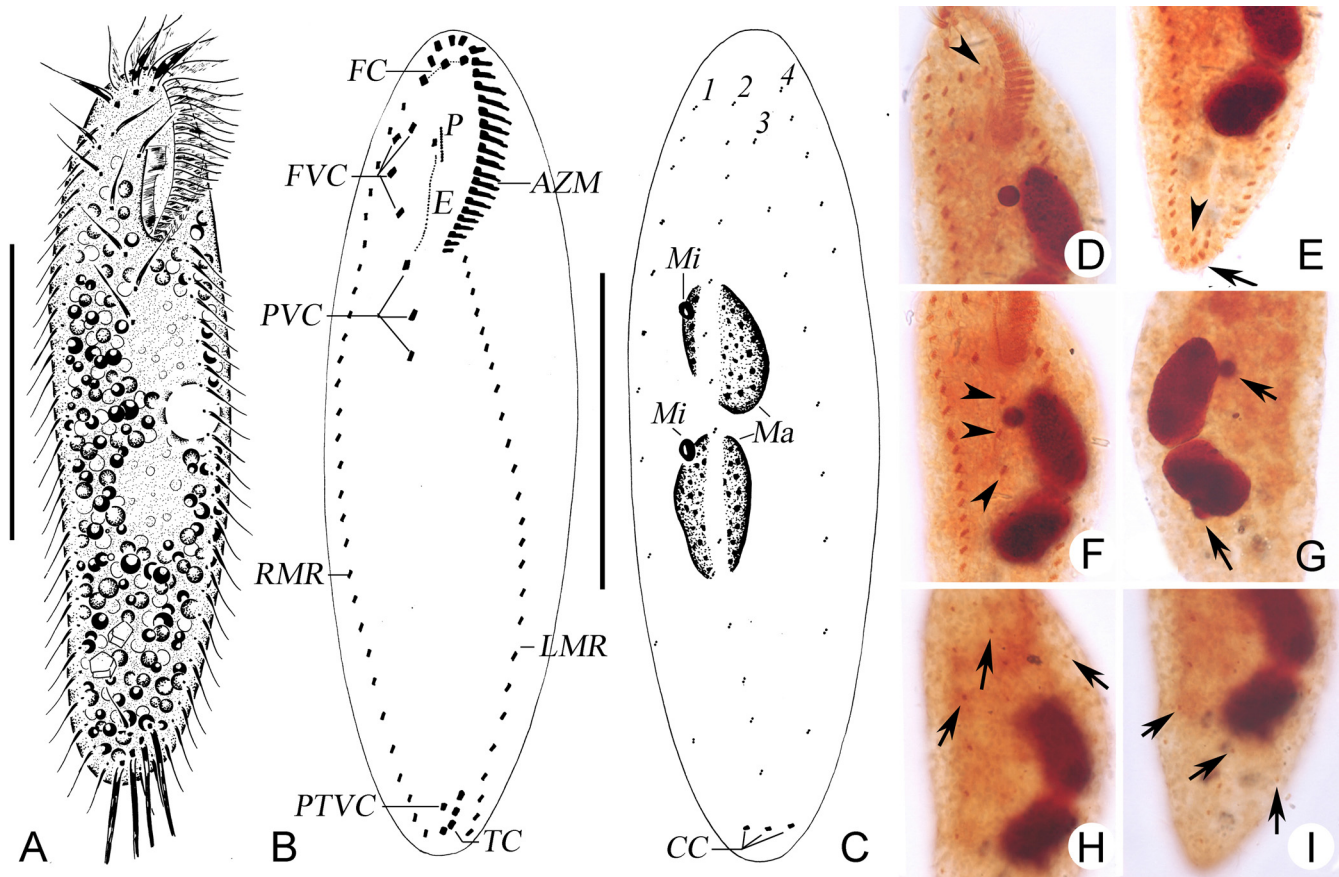


Fig. 2. Morphology of *Urosoma salmastra* from life (A) and staining with protargol (B–I) (D–I from the same cell). (A) Ventral view of a representative individual. (B, C) Ventral (B) and dorsal (C) view, showing the infraciliature. (D) Ventral view of anterior part, arrowhead indicates buccal cirrus. (E) Ventral view of posterior part, showing transverse cirri (arrow) and pretransverse cirrus (arrowhead). (F, G) Ventral (F) and dorsal (G) view of middle part, demonstrating postoral ventral cirri (arrowheads), macronuclear nodules and micronuclei (arrows). (H, I) Dorsal views, showing dorsal kinetics (arrows). AZM, adoral zone of membranelles; CC, caudal cirri; E, endoral; FC, frontal cirri; FVC, frontoventral cirri; LMR, left marginal row; Ma, macronuclear nodules; Mi, micronuclei; P, paroral; PTVC, pretransverse ventral cirri; PVC, postoral ventral cirri; RMR, right marginal row; TC, transverse cirri; 1–4, dorsal kinetics. Scale bars = 50 µm.

(Fig. 1C, D). The Sangke Grass land is mostly over 3000 m above sea level. The annual temperature is 2 °C and annual precipitation is 650 mm. There are, on average, 20–40 vascular plant species per 0.25 m². The vegetation is dominated by *Kobresia graminifolia*, *Poa botryoides*, *Elymus nutans*, *Anemone rivularis*, and others. The sample comprised 500 g of soil from the top 10 cm layer. Ciliates were stimulated to excyst and emerge from the soil samples by employing the non-flooded Petri dish method described by Foissner (1987a) and Foissner et al. (2002). Isolated specimens were maintained as non-clonal cultures in Petri dishes at room temperature (20 °C) using boiled freshwater with rice grains to enrich bacterial food organisms.

Morphology

Living cells were observed using bright field and differential interference contrast microscopy. The protargol silver

staining method according to Wilbert (1975) was used to reveal the infraciliature. Measurements of silvered specimens were carried out with an ocular micrometre. Drawings of silvered specimens were performed at 1250× magnification with the aid of a camera lucida.

Terminology

General terminology is mainly according to Berger (1999); for explanation of terms specific for hypotrichs (e.g., Gonostomum-pattern, Urosomoida-pattern, pseudorow, mixed row, DE-value), see Berger and Foissner (1997), Berger (1999, 2006, 2008, 2011), Foissner and Al-Rasheid (2006), and Foissner and Stoeck (2011). The numbering system of Wallengren (1900) was used for the designation of the frontoventral-transverse cirri (for details, see Berger 1999: 16). The term ‘18-cirri hypotrich’ means a hypotrich with 18 frontal–ventral–transverse cirri (Berger 2008: 27).

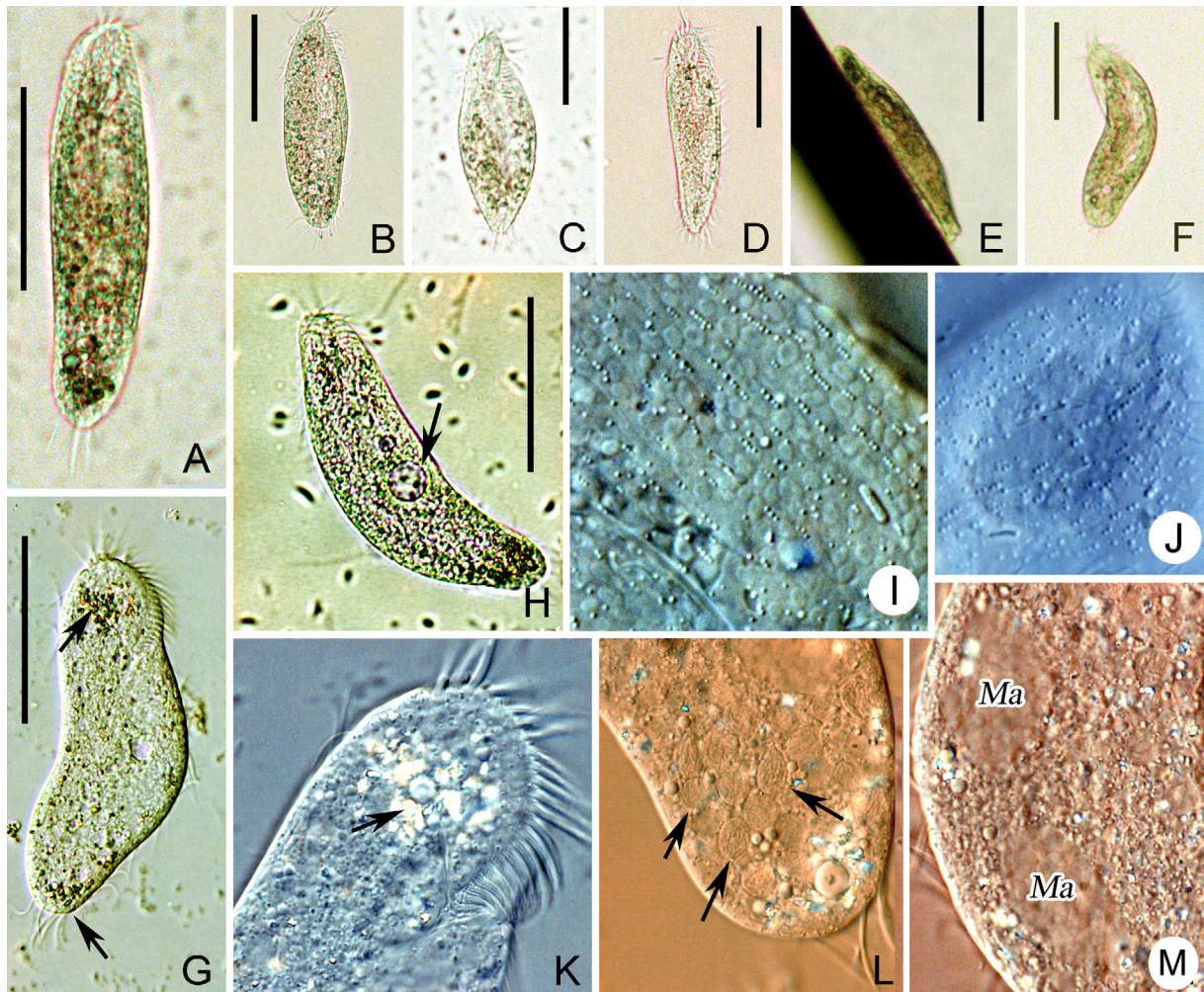


Fig. 3. Photomicrographs of *Urosoma salmastra* from life. (A) Ventral view of a typical cell. (B–D) Ventral views of other individuals, to show different body shapes. Individual shown in (C) is a divider. (E) Lateral view, to show dorsal–ventrally flattened body. (F) Bending individual, showing the flexibility of the body. (G) A squeezed individual, arrows mark groups of crystals at both ends of cell. (H) Ventral view, arrow indicates contractile vacuole. (I, J) Dorsal views, demonstrating cortical granules in irregular short lines. (K) Ventral view of anterior portion, to show crystals (arrow). (L) Posterior end of cell, showing food vacuoles (arrows). (M) Macronuclear nodules. Ma, macronuclear nodules. Scale bars = 70 μm .

DNA extraction, PCR amplification, and sequencing

For each taxon one or more cells were isolated and washed three times with sterilized water (0.22 μm filtered) in order to remove potential contamination. They were then transferred to a 1.5 ml microfuge tube with a minimum volume of water, and genomic DNA was extracted using a RED Extract-N-Amp Tissue PCR Kit (Sigma, St. Louis, MO). The small subunit (SSU) rRNA gene sequence was amplified by polymerase chain reaction (PCR) using the eukaryotic universal primers EukA (5'-AAC CTG GTT GAT CCT GCC AGT-3') and EukB (5'-TGA TCC TTC TGC AGG TTC ACC TAC-3') (Medlin et al. 1988). Cycling parameters for PCR amplification were according to Yi and Song (2011). To minimize the

possibility of amplification errors, high-fidelity Taq (Takara Ex Taq; Takara Biomedicals, Dalian, China) was used. The PCR product of approximately 1.8 kb in length was purified using SanPrep DNA Gel Extraction Kit (Sangon Bio. Co., Shanghai, China) and was then sequenced bidirectionally on an ABI 3700 sequencer (Invitrogen sequencing facility, Shanghai, China).

Phylogenetic analyses

Using MUSCLE v3.7 (Edgar 2004), the SSU rRNA gene sequences of *Urosoma salmastra* and *U. kariniae sinense* nov. ssp. were aligned to 40 hypotrichid sequences obtained from GenBank database. These sequences were edited manually using Bioedit 7.0 in order to remove the

Table 1. Characterization of *Urosoma salmastra* (upper line, Benin population from Dragesco and Dragesco-Kernéis 1986; lower line, Chinese population).

Character ^a	Min	Max	Mean	SD	CV	n
Body length	48	101	73.0	—	—	29
	84	142	120.0	15.5	12.9	20
Body width	15	30	21.0	—	—	27
	22	59	40.1	10.5	26.2	20
Adoral zone, length	—	—	19.8 ^b	—	—	1
	27	43	34.7	5.0	14.4	20
Adoral membranelles no.	21	26	23.0	—	—	17
	19	25	23.5	1.4	5.9	20
Buccal cirri no.	—	—	1.0 ^b	—	—	1
	1	1	1.0	0	0	20
Frontal cirri no.	—	—	3.0 ^b	—	—	1
	3	3	3.0	0	0	20
Frontoventral cirri no.	—	—	4.0 ^b	—	—	1
	4	4	4.0	0	0	20
Postoral ventral cirri no.	—	—	3.0 ^b	—	—	1
	3	3	3.0	0	0	20
Pretransverse ventral cirri no.	—	—	1.0	—	—	?
	1	2	1.1	0.3	28.0	20
Transverse cirri no.	3	5	4.0	—	—	7
	3	4	3.7	0.5	12.7	20
Cirri in left marginal row no.	16	25	21.0	—	—	20
	21	31	23.5	2.6	11.0	20
Cirri in right marginal row no.	22	30	26.0	—	—	24
	19	39	25.0	5.0	20.2	20
Caudal cirri no.	—	—	3.0 ^b	—	—	1
	3	3	3.0	0	0	20
Dorsal kineties no.	—	—	4.0 ^b	—	—	1
	4	4	4.0	0	0	20
Dorsal kinety 1, bristles no.	—	—	11.0 ^b	—	—	1
	10	11	—	—	—	3
Dorsal kinety 2, bristles no.	—	—	10.0 ^b	—	—	1
	11	13	—	—	—	3
Dorsal kinety 3, bristles no.	—	—	10.0 ^b	—	—	1
	9	10	—	—	—	3
Dorsal kinety 4, bristles no.	—	—	4.0 ^b	—	—	1
	5	6	—	—	—	3
Macronuclear nodules no.	—	—	2.0 ^b	—	—	1
	2	2	2.0	0	0	20
Micronuclei no.	—	—	2.0 ^b	—	—	1
	1	4	2.0	0.7	36.3	20
Macronuclear nodule, length	—	—	11.8 ^b	—	—	1
	19	39	25.0	5.0	20.2	20
Macronuclear nodule, width	—	—	8.3 ^b	—	—	1
	7	17	11.1	3.1	27.7	20

^aAll data are based on protargol-stained specimens. Measurements in μm . Abbreviations: CV, coefficient of variation in %; Max, maximum; Mean, arithmetic mean; Min, minimum; n, number of cells measured; SD, standard deviation. —, data unavailable.

^bData from drawings.

ambiguous regions (Hall 1999), resulting in a matrix of 1722 nucleotide characters. Three urostylid species, namely *Urostyla grandis*, *Uroleptopsis citrina* and *Apobakuella fusca*, were selected as the outgroup taxa. MrModeltest v.2.0 (Nylander 2004) selected the GTR + I ($=0.6336$) + G ($=0.4830$) as the best model with Akaike information criterion (AIC), which was then used for Bayesian (BI) analyses. A Bayesian inference (BI) analysis was performed with MrBayes 3.1.2 (Ronquist and Huelsenbeck 2003), with a run of 1,000,000 generations at a sampling frequency of 100. The first 25% of sampled trees was discarded as “burn-in”. For the remaining trees, a 50% majority rule consensus tree was used to calculate posterior probability values for BI. Maximum Likelihood (ML) analyses were performed online on the CIPRES Science Gateway (The CIPRES Portals. URL: <http://www.phylo.org/sub-sections/portal>) with RaxML-HPC BlackBox (7.2.8) (Stamatakis et al. 2008). Nodal support came from 1000 bootstrap replicates. TREEVIEW v1.6.6 (Page 1996) and MEGA 4.0 (Tamura et al. 2007) were used to visualize tree topologies.

Results

Urosoma salmastra (Dragesco and Dragesco-Kernéis, 1986) Berger, 1999 (Figs 2A–I, 3A–M, Table 1)

Improved diagnosis (based on original description and data on Chinese population)

Body outline elongate-elliptical, $110\text{--}150\ \mu\text{m} \times 30\text{--}50\ \mu\text{m}$ in vivo (about $50\text{--}140\ \mu\text{m} \times 15\text{--}60\ \mu\text{m}$ in protargol preparations). Cortical granules colourless, less than $1\ \mu\text{m}$ across, arranged in longitudinally oriented short rows. Two macronuclear nodules and usually two micronuclei. One contractile vacuole located at midbody near left body margin. Adoral zone spans 25% of body length in vivo (about 30% in protargol preparations) and composed of about 23 membranelles on average. Paroral very short, located in front of endoral. Usually 16 frontoventral transverse cirri. Marginal rows normally separated posteriorly. Dorsal kinetics 1–3 bipolar, kinety 4 terminating at one-third of cell length. Three caudal cirri, almost indistinguishable from dorsal bristles when viewed in vivo.

Description of *U. salmastra* based on Chinese population

Body size in vivo $110\text{--}150\ \mu\text{m} \times 30\text{--}50\ \mu\text{m}$, length:width ratio approximately 3:1. Body outline elongate-elliptical with both ends widely rounded; right cell margin almost straight, left margin slightly to distinctly convex (Figs 2A, 3A–D). Body usually widest ahead of mid-body; dorsoventrally flattened about 2:1; flexible but not distinctly contractile (Fig. 3E, F). Contractile vacuole about $10\text{--}15\ \mu\text{m}$ in

diameter when full, located in midbody region near left margin (Figs 2A, 3H). Cortical granules spherical, less than $1\ \mu\text{m}$ across, colourless, arranged in longitudinally oriented short rows (Fig. 3I, J). Cytoplasm hyaline and colourless, frequently containing many lipid droplets $2\text{--}3\ \mu\text{m}$ across, food vacuoles $8\text{--}10\ \mu\text{m}$ across, and crystals that render cell opaque and dark at low magnification (Figs 2A, 3A, G, K, L). Two macronuclear nodules usually arranged along cell midline, or slightly left of it, behind buccal vertex; nodules ellipsoidal (length:width ratio about 2–2.5:1), with small to moderately large nucleoli (Figs 2A, C, 3M). Usually one micronucleus attached to each macronuclear nodule (Fig. 2G). Locomotion by continuous, slow to moderately fast crawling on bottom of Petri dish. When suspended, cells often swim continuously in circles.

Adoral zone of membranelles about 25% of body length in vivo, but 29% on average in protargol preparations due to strong cell expansion caused by the fixative (Fig. 2B). Infra-ciliature as shown in Fig. 2B–F, H, I. Adoral zone composed of 19–25 membranelles in typical *Gonostomum*-pattern (i.e. middle portion of adoral zone straight, aligned with left margin of cell, causing proximal part of adoral zone to become abruptly bent towards centre of body). Distal portion of adoral zone extends slightly posteriorly onto right side of cell, i.e. DE-value 0.14 (Fig. 2B; for explanation of DE-value, see Berger 2006: 18). Paroral and endoral roughly in *Gonostomum*-pattern (paroral very short and located in front of endoral, Fig. 2B). Buccal lip slightly curved, covering only right part of proximal portion of adoral zone (Fig. 2A).

Usually 16 frontoventral-transverse cirri (Fig. 2B). All cirri relatively fine, about $10\text{--}12\ \mu\text{m}$ long in vivo except for frontal and transverse cirri which are about $15\ \mu\text{m}$ long. Frontal cirri slightly larger than frontoventral cirri, arranged in oblique pseudorow with right cirrus (=III/3) immediately posterior to distal end of adoral zone. Buccal cirrus located to right of mid-region of paroral and in front of endoral (Fig. 2B, D). Parabuccal cirrus (=III/2) immediately posterior of right frontal cirrus, anterior to level of cirrus VI/4 and closer to remaining frontoventral cirri than to undulating membranes (Fig. 2B, D). Remaining three frontoventral cirri, i.e. two frontoterminal cirri and cirrus IV/3, form a short row. Postoral ventral cirri arranged in a line, anteriormost cirrus at level of buccal vertex (Fig. 2B, F). Pretransverse ventral cirrus(i) close to transverse cirri (Fig. 2B, E). Transverse cirri form roughly J-shaped pseudorow and only slightly displace anteriad, therefore cirri project three-quarters of their length beyond posterior body margin. One right and one left marginal row, posterior ends of which are separated by an $8\ \mu\text{m}$ wide gap; left row with 21–31 cirri, right row with 19–39 cirri.

Dorsal bristles about $3\ \mu\text{m}$ long in life, always arranged in four kinetics. Kinetics 1–3 extending nearly whole body length, kinety 4 terminating at about 33% of body length (Fig. 2C, H, I). Three caudal cirri at posterior margin of body, about $15\ \mu\text{m}$ long in vivo and thus almost indistinguishable from marginal cirri (Fig. 2C).

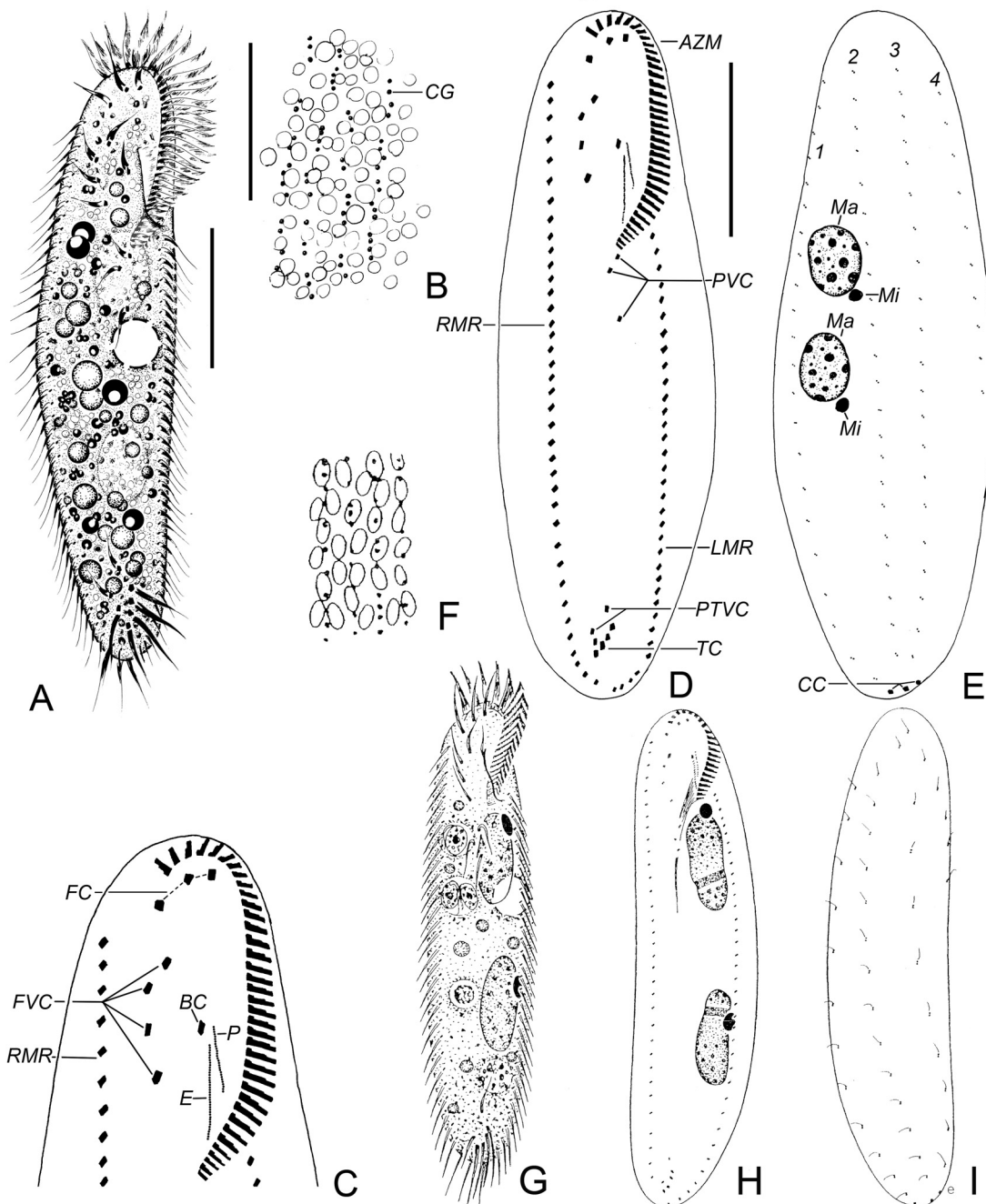


Fig. 4. Morphology of *Urosoma karinae sinense* nov. ssp. (A–E) and *U. karinae karinae* (F–I, from Foissner 1987b) from life (A, B, F, G) and staining with protargol (C–E, H, I). (A, G) Ventral view of a representative individual. (B, F) Cortical granules in irregular short lines (arrows) and mitochondria. (C) Ventral view of anterior part. (D, E, H, I) Ventral (D, H) and dorsal (E, I) view of same specimens, showing the infraciliature. AZM, adoral zone of membranelles; BC, buccal cirrus; CC, caudal cirri; CG, cortical granules; E, endoral; FC, frontal cirri; FVC, frontoventral cirri; LMR, left marginal row; Ma, macronuclear nodules; Mi, micronuclei; P, paroral; PTVC, pretransverse ventral cirri; PVC, postoral ventral cirri; RMR, right marginal row; TC, transverse cirri; 1–4, dorsal kineties. Scale bars: A, D, E=50 µm, B=35 µm.

Deposition of material

Two voucher slides with protargol-stained specimens of *Urosoma salmastra* are deposited in the Laboratory of Protozoology, OUC, China, with registration numbers

PY10112502-01 and -02 and one voucher slide with protargol-impregnated specimens is deposited in the Natural History Museum, London (registration number NHMUK 2013.12.16.1).

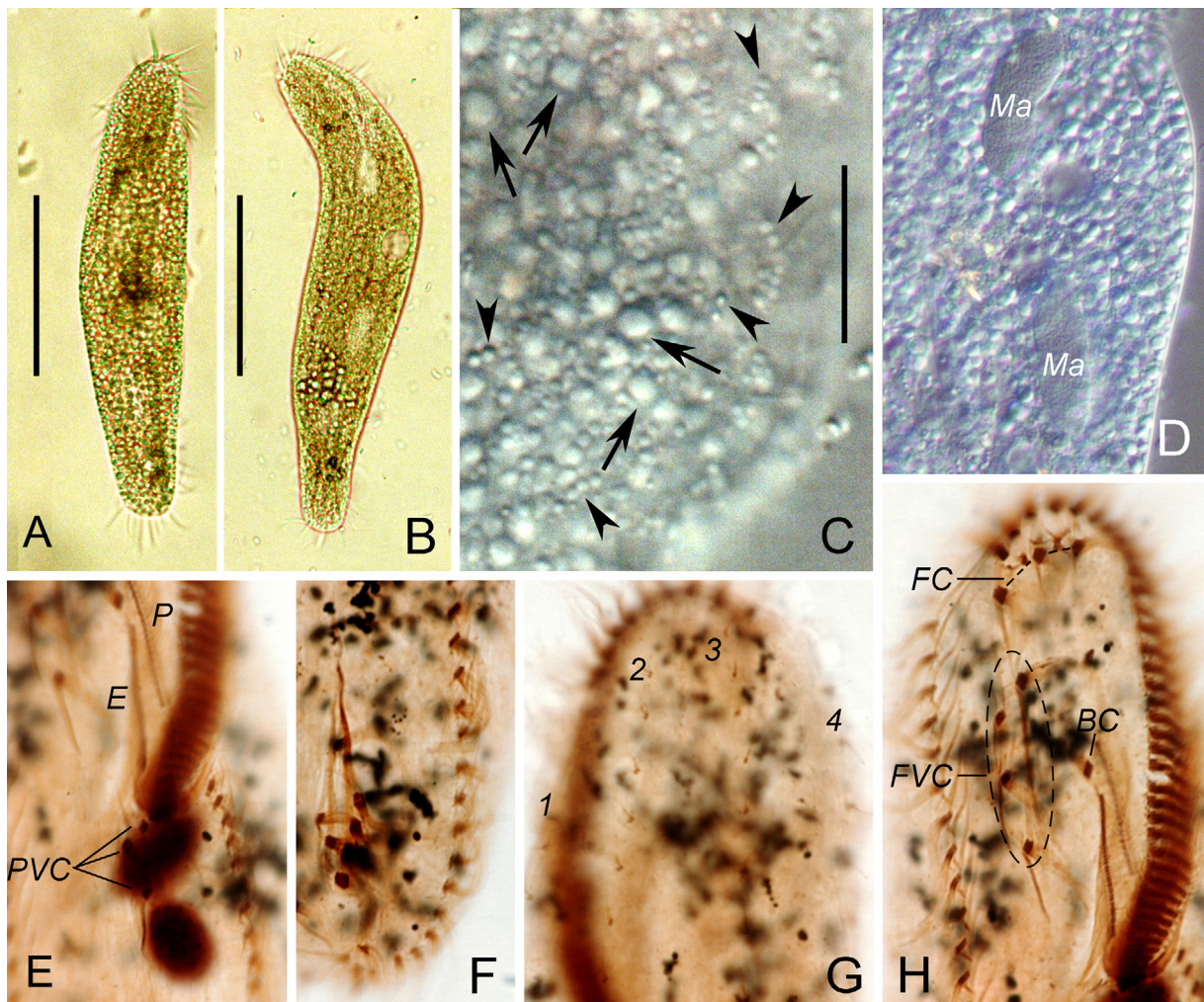


Fig. 5. Photomicrographs of *Urosoma karinae sinense* nov. ssp. from life (A–D) and staining with protargol (E–H). (A) Ventral view of a typical cell. (B) Bending individual, showing flexibility of body. (C) Dorsal view, demonstrating cortical granules in irregular short lines (arrowheads) and mitochondria (arrows). (D) Macronuclear nodules. (E) Ventral view of oral region showing undulating membranes and postoral ventral cirri. (F) Posterior end of cell, showing transverse and pretransverse cirri. (G) Dorsal view of anterior portion, to show dorsal kineties. (H) Ventral view of the anterior portion, to show the frontal, frontoventral and buccal cirri. BC, buccal cirrus; E, endoral; FC, frontal cirri; FVC, frontal ventral cirri; Ma, macronuclear nodules; P, paroral; PVC, postoral ventral cirri; 1–4, dorsal kineties. Scale bars: A, B = 50 µm; C = 15 µm.

Urosoma karinae sinense nov. ssp. (Figs 4A–E, 5A–H, Table 2)

Diagnosis

With characters of *U. karinae* but numbers of dikinetids in dorsal kineties 1, 2, 3 and 4 about 22, 22, 21 and 10, respectively.

Type locality

Upper 10 cm layer of soil collected from the Sangke Grass Land ($35^{\circ}06' N$; $102^{\circ}25' E$), Gansu Province, China.

Type material

The slide (No. CLY11102401-01) containing the holotype specimen (Fig. 4D, E) and a paratype slide (No.

CLY11102401-02) with protargol-impregnated specimens are deposited in the Laboratory of Protozoology, OUC, China. One paratype slide with protargol-stained specimens is deposited in the Natural History Museum, London (registration number NHMUK 2013.12.16.2).

Etymology

Named after the country discovered.

Description

Body 150–250 µm × 45–50 µm in vivo, elongate-elliptical with right margin slightly convex and left margin more or less straight; both ends rounded; flexible but not contractile (Figs 4A, 5A). Cells frequently with many lipid droplets 2–4 µm across and food vacuoles 2–5 µm across. Posterior region with many crystals rendering this part of

Table 2. Characterization of *Urosoma karinae sinense* nov. ssp. (upper line) and *Urosoma karinae karinae* Foissner, 1987 (lower line, from Foissner 1987b).

Character ^a	Min	Max	Mean	SD	CV	n
Body length	138	230	186.8	25.8	13.8	20
	92	154	119.2	18.1	15.2	10
Body width	38	72	50.3	8.5	17.0	20
	29	42	36.1	4.6	12.7	10
Adoral zone, length	38	72	50.3	8.5	17.0	20
	21	29	25.1	2.6	10.4	10
Adoral membranelles no.	30	42	36.1	3.1	8.7	20
	21	24	22.0	1.0	4.5	10
Buccal cirri no.	1	1	1.0	0	0	20
	1	1	1.0	0	0	10
Frontal cirri no.	3	3	3.0	0	0	20
	3	4	3.1	-	-	10
Frontoventral cirri no.	4	4	4.0	0	0	20
	4	4	4.0	0	0	10
Postoral ventral cirri no.	2	3	2.9	0.3	8.5	16
	1	2	1.0	-	-	10
Pretransverse ventral cirri no.	2	2	2.0	0	0	20
	1	2	1.1	0.3	28.7	10
Transverse cirri no.	5	5	5.0	0	0	20
	5	5	5.0	0	0	10
Cirri in left marginal row no.	21	44	35.1	6.2	17.7	20
	26	36	30.4	3.4	11.3	10
Cirri in right marginal row no.	25	48	37.5	5.4	14.3	20
	26	33	29.2	2.3	8.0	10
Caudal cirri no.	2	5	3.3	0.8	23.8	16
	3	3	3.0	0	0	10
Dorsal kineties no.	4	4	4.0	0	0	13
	4	4	4.0	0	0	10
Dorsal kinety 1, bristles no.	20	23	22.1	0.9	4.0	10
	8?	12?	-	-	-	4
Dorsal kinety 2, bristles no.	20	24	22.4	1.4	6.4	10
	11?	15?	-	-	-	4
Dorsal kinety 3, bristles no.	20	23	21.4	1.1	5.0	10
	9?	10?	-	-	-	4
Dorsal kinety 4, bristles no.	9	12	10.4	1.3	13.0	10
	5?	7?	-	-	-	4
Macronuclear nodules no.	2	4	2.1	0.5	21.3	20
	2	3	2.0	-	-	10
Micronuclei no.	1	4	2.4	1.1	47.5	5
	1	3	2.0	0.7	33.3	10
Macronuclear nodule, length	15	39	27.1	7.3	26.8	19
	18	31	23.1	4.3	18.5	10
Macronuclear nodule, width	7	16	10.9	3.0	27.5	19
	7	11	9.4	1.5	16.0	10

^aAll data are based on protargol-stained specimens. Measurements in µm. Abbreviations: CV, coefficient of variation in %; Max, maximum; Mean, arithmetic mean; Min, minimum; n, number of cells measured; SD, standard deviation. -, data unavailable; ?, value not quite certain because kineties not very well stained.

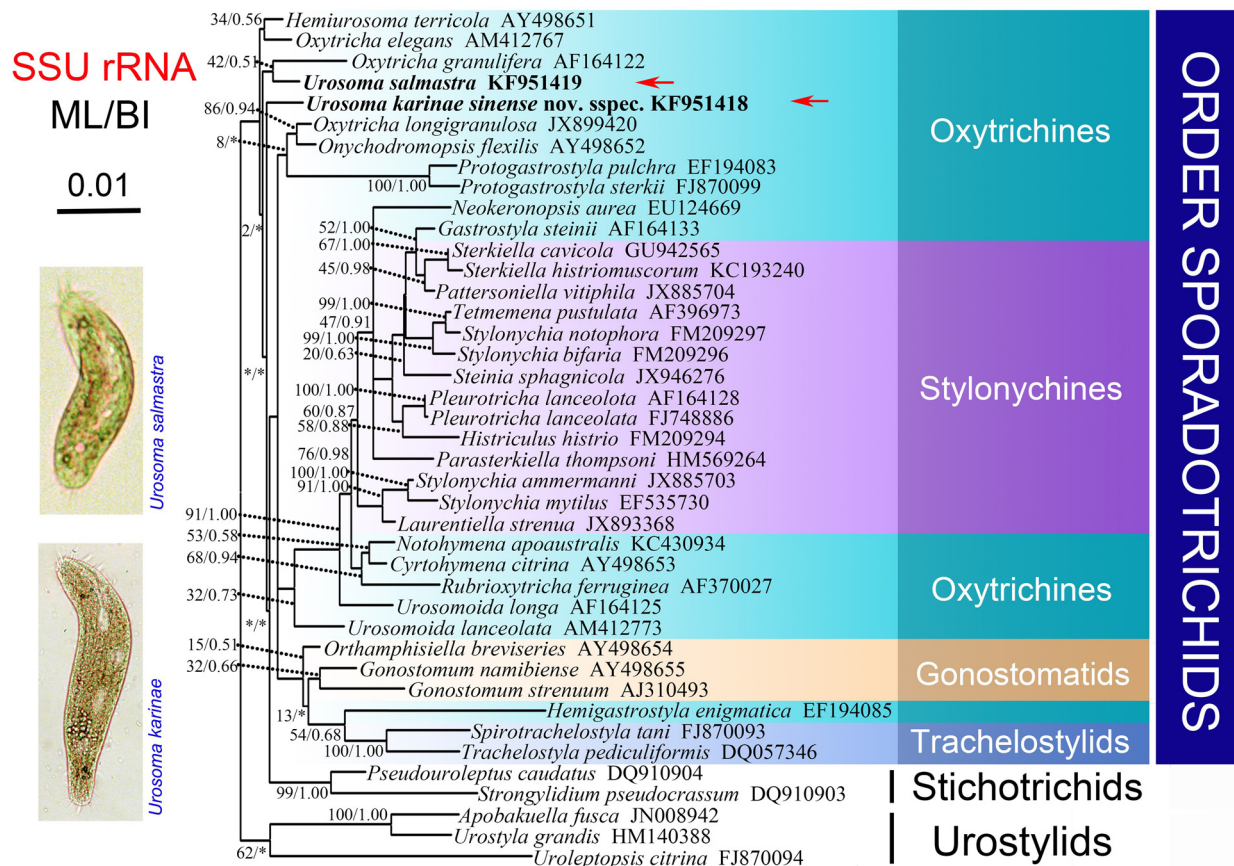


Fig. 6. Maximum likelihood (ML) phylogenetic tree inferred from the small subunit ribosomal RNA gene sequences of 42 hypotrichs showing the position of *Urosoma salmastra* and *U. kariniae sinense* nov. sspe. Numbers near nodes are nonparametric bootstrap values for ML and posterior probability values for Bayesian inference (BI). “*” refers to disagreement in topology with the BI tree. All branches are drawn to scale. The scale bar corresponds to 0.01 expected substitutions per site.

cell dark at low magnification when viewed with bright field illumination. Contractile vacuole measuring 15–20 µm when fully expanded, located in midbody region near left margin, contracting at intervals of 5–8 s (Fig. 4A). Cortical granules less than 1 µm across, colourless, arranged in short, irregular, longitudinally oriented rows, easily distinguishable from mitochondria which are ellipsoidal, 4–5 µm across (Figs 4B, 5C). Two (rarely three or four) macronuclear nodules usually located in mid-body region left of cell midline; nodules ellipsoidal, 15–39 µm × 7–16 µm after staining with protargol, with small to moderately large nucleoli (Figs 4E, 5B, D). One to four (usually two) micronuclei, 6 µm × 4 µm after staining with protargol (Fig. 4E). Locomotion by continuous, slow crawling on bottom of Petri dish or on surface of water.

Infraciliature as shown in Figs 4C–E, 5E–H. Adoral zone about 30% of body length in vivo, composed of 30–42 membranelles in typical *Gonostomum*-pattern. Distal portion of adoral zone extends slightly posteriorly onto right side of cell; DE-value <0.1 (Fig. 4C). Paroral shorter than, and located in front of, endoral (Figs 4C, 5E). Buccal lip slightly curved, covering only right part of proximal portion of adoral zone (Fig. 4A).

Frontoventral-transverse ciliation comprises 18 cirri. Three slightly enlarged frontal cirri with cilia about 15 µm long, arranged in oblique pseudorow with right cirrus (=III/3) posterior to distal end of adoral zone (Figs 4C, 5H). Single buccal cirrus right of anterior end of paroral and anterior to endoral (Figs 4, 5H). Parabuccal cirrus (=III/2) immediately posterior to right frontal cirrus, anterior to level of cirrus VI/4 (Figs 4C, 5H). Remaining three frontoventral cirri (two frontoterminal cirri and cirrus IV/3) form a short row (Figs 4C, 5H). Three (rarely two) postoral ventral cirri located immediately posterior to buccal vertex and distinctly separated from two pre-transverse ventral cirri; postoral ventral cirrus IV/2 located anterior to V/4 (Figs 4D, 5E). Five transverse cirri in hook-shaped pseudorow, with cilia about 20 µm long in vivo (Figs 4D, 5F). Two pretransverse ventral cirri with cirrus VI/2 located at about same level as leftmost transverse cirrus (Figs 4D, 5F). One right and one left marginal row, posterior ends of which almost confluent; left row with 21–44 cirri, right row with 25–48 cirri; cilia of marginal cirri about 12 µm long in vivo (Fig. 4D).

Four dorsal kineties; leftmost three (dorsal kineties 1–3) bipolar, each comprising about 20 pairs of basal bodies; dorsal kinety 4 starts near anterior end of cell and terminates at

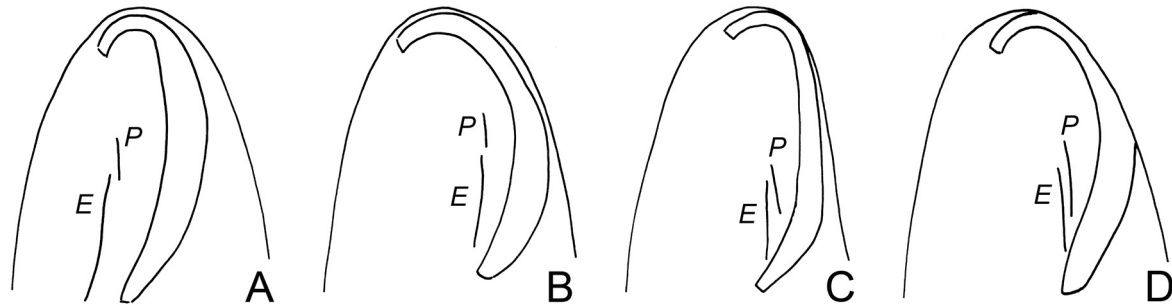


Fig. 7. A–D. Comparison of various paroral and endoral patterns of *Urosoma salmastra* and *U. karinae*. (A) *U. salmastra* (Chinese population). (B) *U. salmastra* (from Dragesco and Dragesco-Kernéis 1986). (C) *U. karinae sinense* nov. ssp. (D) *U. karinae karinae* Foissner, 1987 nov. stat. (from Foissner 1987b). E, endoral; P, paroral.

about midbody (Figs 4E, 5G). Dorsal cilia about 3 µm long in vivo. Three caudal cirri located at posterior body margin, one each at posterior end of dorsal kineties 1, 2, and 3; cilia of caudal cirri about 20 µm long in vivo (Fig. 4E).

Urosoma karinae karinae Foissner, 1987 nov. stat.

Diagnosis

With characters of *U. karinae* but with numbers of dakinetids in =dorsal kineties 1, 2, 3 and 4 about 11, 13, 9 and 6, respectively.

Description

For detailed description and revision of the nominotypical subspecies, see Foissner (1987b) and Berger (1999).

SSU rRNA gene sequences and phylogenetic analyses

The SSU rRNA gene sequences of both taxa have been deposited in GenBank. The length and accession number of each is as follows: *Urosoma salmastra* (1774 bp, KF951419) and *U. karinae sinense* nov. ssp. (1758 bp, KF951418). The G + C content of the two taxa were 45.72% and 44.88% respectively. The topologies of the ML and BI trees were similar, therefore only the ML tree is shown (Fig. 6). In both analyses, *U. salmastra* and *Oxytricha granulifera* clustered with low support (ML/BI, 42/0.51) and formed a sister clade to the large clade including *U. karinae sinense* nov. ssp. with a rather low support. The SSU rRNA gene sequence similarity between *U. salmastra* and *U. karinae sinense* nov. ssp. is 96.6%.

Discussion

Urosoma salmastra (Dragesco and Dragesco-Kernéis, 1986) Berger, 1999

Comparison with Benin population

Based on the original report of *Urosoma salmastra* isolated from Benin, Africa (Dragesco and Dragesco-Kernéis 1986), our population from China closely resembles the Benin

population in all key characters, i.e. shape, nuclear apparatus, arrangement of frontoventral cirri, pattern of paroral and endoral, length of dorsal kinety 4, morphometric data (Fig. 7, Table 1, Berger 1999) and biotope (saline). Therefore, the identity of the Zhanjiang population is not in doubt.

Urosoma karinae sinense nov. ssp.

Comparison with *Urosoma karinae karinae* Foissner, 1987 nov. stat.

Urosoma karinae karinae nov. stat. was described from a population isolated in Salzburg, Austria (Foissner 1987b). *Urosoma karinae sinense* nov. ssp. closely resembles *U. karinae karinae* Foissner, 1987 nov. stat. apart from slight differences in the number of transverse cirri (5 vs. 3 or 4 in *U. karinae karinae* nov. stat.) and total number of dorsal bristles (about 76 vs. about 38 in *U. karinae karinae* nov. stat.) (Foissner 1987b). We consider that these differences could be intra-specific because the localities of these two populations are very widely separated and there was significant difference between the two habitats from which the populations of *U. karinae karinae* and *U. karinae sinense* were isolated, i.e. altitude (1270 m vs. 3000 m). Since all other key characters, i.e. body size, shape, macronuclear features, arrangement of endoral and paroral, morphometric data (Fig. 7, Table 2) and biotope (soil), are consistent with the original description, we believe the two are conspecific and erect a new subspecies for the Chinese population.

Comparison of *Urosoma salmastra* and *U. karinae* with congeners

In terms of its elongate-elliptical body with no tail and two macronuclear nodules, one congener, namely *Urosoma gigantea*, should be compared with *U. salmastra* and *U. karinae*. *Urosoma gigantea* (Horváth, 1933) Berger, 1999 resembles *U. salmastra* in terms of its body shape and cortical granules but can be distinguished from the latter by having a larger body size (170–230 µm vs. 110–150 µm), an adoral zone that is longer relative to the body length (37% vs. ca. 25%), cirrus III/2 located between cirri VI/3 and VI/4

(vs. ahead of the level of VI/4), paroral and endoral with equal length (vs. endoral significantly longer than paroral), more pretransverse cirri (2 vs. 1), more dikinetids in dorsal kinety 1 (29, based on drawing vs. 11) and five transverse cirri arranged in an asymmetric V-shaped pseudorow (vs. 3 or 4 arranged in a J-shaped pseudorow) (Berger 1999).

Urosoma gigantea can be separated from *U. karinae* by having an adoral zone that is rather long relative to the body length (37% vs. ca. 30%) and cirrus III/2 located between cirri VI/3 and VI/4 (vs. ahead of the level of VI/4) (Berger 1999).

Compared with the *Urosoma karinae* Foissner, 1987, *U. salmastra* has a paroral that is much shorter than, and located ahead of, the endoral (vs. paroral and endoral in parallel and of equal length in *Urosoma karinae*), fewer pretransverse cirri (1 vs. 2) and total number of dorsal bristles (ca. 37 in *U. salmastra* vs. ca. 76 in *U. karinae sinense*) (Fig. 7, Berger 1999; Foissner 1987a,b). The divergence of these two taxa is also firmly supported by the molecular data, the SSU rRNA gene sequence similarity being only 96.6%.

Phylogeny

Urosoma salmastra was most closely associated with *O. granulifera* in all trees, with *U. karinae sinense* branching basally to them. This clade was an essentially unresolved group of sequences within the oxytrichine assemblage of the family Oxytrichidae. Species of *Oxytricha* did not appear to form a monophyletic group, suggesting that diagnostic characters of the genus might have evolved convergently in different lineages (Shao et al. 2011). The apparent polyphyly of *Oxytricha* may also be due to the limited number of taxa that have been sequenced. As more species of the family Oxytrichidae are described and sequenced, a more robust phylogeny may be obtained. Furthermore, some other gene sequences (e.g. ITS, LSU rDNA, tubulin) may provide additional information for determining the evolutionary relationships within this group (Huang et al. 2012, 2014; Miao et al. 2011; Yi et al. 2012).

Acknowledgements

This work was supported by the Natural Science Foundation of China (Project numbers: 31372148 to C. Shao, 31272285 to M. Miao) and the Fundamental Research Funds for the Central Universities. Many thanks are due to Dr. Berger for kindly examining the dorsal ciliature of *Urosoma karinae karinae*.

References

Berger, H., 1999. Monograph of the Oxytrichidae (Ciliophora, Hypotrichia). Monogr. Biol. 78, 1–1080.

- Berger, H., 2006. Monograph of the Urostyloidea (Ciliophora, Hypotrichia). Monogr. Biol. 85, 1–1303.
- Berger, H., 2008. Monograph of the Amphisellidae and Trachelostylidae (Ciliophora, Hypotrichia). Monogr. Biol. 88, 1–737.
- Berger, H., 2011. Monograph of the Gonostomatidae and Kahliidae (Ciliophora, Hypotrichia). Monogr. Biol. 90, 1–741.
- Berger, H., Foissner, W., 1997. Cladistic relationships and generic characterization of oxytrichid hypotrichs (Protozoa, Ciliophora). Arch. Protistenkd. 148, 125–155.
- Chen, X., Shao, C., Lin, X., Clamp, J.C., Song, W., 2013a. Morphology and molecular phylogeny of two new brackish-water species of *Amphisabella* (Ciliophora, Hypotrichia), with notes on morphogenesis. Eur. J. Protistol. 49, 453–466.
- Chen, X., Yan, Y., Hu, X., Zhu, M., Ma, H., Warren, A., 2013b. Morphology and morphogenesis of a soil ciliate, *Rigidohymena candens* (Kahl, 1932) Berger, 2011 (Ciliophora, Hypotrichia, Oxytrichidae), with notes on its molecular phylogeny based on SSU rDNA sequence data. Int. J. Syst. Evol. Microbiol. 63, 1912–1921.
- Dragesco, J., Dragesco-Kernéis, A., 1986. Ciliés libres de l'Afrique intertropicale. Introduction à la connaissance et à l'étude des ciliés. Faune Tropicale 26, 1–559.
- Edgar, R.C., 2004. Muscle: multiple sequence alignment with high accuracy and high throughput. Nucleic Acids Res. 32, 1792–1797.
- Foissner, W., 1987a. Soil protozoa: fundamental problems, ecological significance, adaptations in ciliates and testaceans, bioindicators, and guide to the literature. Progr. Protistol. 2, 69–212.
- Foissner, W., 1987b. Faunistische und taxonomische Notizen über die Protozoen des Fuscher Tales (Salzburg Österreich). Jber. Haus Nat. Salzburg 10, 56–68.
- Foissner, W., Al-Rasheid, K., 2006. A unified organization of the stichotrichine oral apparatus, including a description of the buccal seal (Ciliophora: Spirotrichea). Acta Protozool. 45, 1–16.
- Foissner, W., Stoeck, T., 2011. *Cotterillia bromelicola* nov. gen., nov. spec., a gonostomatid ciliate (Ciliophora, Hypotrichia) from tank bromeliads (Bromeliaceae) with de novo originating dorsal kinetics. Eur. J. Protistol. 47, 29–50.
- Foissner, W., Agatha, S., Berger, H., 2002. Soil ciliates (Protozoa, Ciliophora) from Namibia (Southwest Africa), with emphasis on two contrasting environments, the Etosha Region and the Namib Desert. Part I: Text and line drawings. Denisia 5, 1–1063.
- Gupta, R., Kamra, K., Sapra, G.R., 2006. Morphology and cell division of the oxytrichids *Architricha indica* nov. gen., nov. sp., and *Histiculus histrio* (Müller, 1773), Corliss, 1960 (Ciliophora, Hypotrichida). Eur. J. Protistol. 42, 29–48.
- Hall, T.A., 1999. BioEdit: a user-friendly biological sequence alignment editor and analysis program for Windows 95/98/NT. Nucleic Acids Symp. Ser. 41, 95–98.
- Huang, J., Dunthorn, M., Song, W., 2012. Expanding character sampling for the molecular phylogeny of euglenoid ciliates (Protozoa, Ciliophora) using three markers, with a focus on the family Uronychiidae. Mol. Phylogenetic Evol. 63, 598–605.
- Huang, J., Chen, Z., Song, W., Berger, H., 2014. Three-gene based phylogeny of the Urostyloidea (Protista, Ciliophora, Hypotrichia), with notes on classification of some core taxa. Mol. Phylogenetic Evol. 70, 337–347.
- Küppers, G.C., Paiva, T.S., Borges, B.N., Harada, M.L., Garraza, G.G., Mataloni, G., 2011. An Antarctic hypotrichous ciliate, *Parasterkiella thompsoni* (Foissner) nov. gen., nov. comb.,

- recorded in Argentinean peat-bogs: morphology, morphogenesis, and molecular phylogeny. *Eur. J. Protistol.* 47, 103–123.
- Li, F., Xing, Y., Li, J., Al-Rasheid, K.A.S., He, S., Shao, C., 2013. Morphology, morphogenesis and small subunit rRNA gene sequence of a soil hypotrichous ciliate, *Perisincirra paucicirrata* (Ciliophora, Kahliellidae), from the shoreline of the Yellow River, north China. *J. Eukaryot. Microbiol.* 60, 247–256.
- Li, L., Huang, J., Song, W., Shin, M.K., Al-Rasheid, K.A.S., Berger, H., 2010. *Apogastrostyla rigescens* (Kahl, 1932) gen. nov., comb. nov. (Ciliophora, Hypotrichida): morphology, notes on cell division, SSU rRNA gene sequence data, and neotypification. *Acta Protozool.* 49, 195–212.
- Lv, Z., Chen, L., Chen, L., Shao, C., Miao, M., Warren, A., 2013. Morphogenesis and molecular phylogeny of a new freshwater ciliate, *Notohymena apoaustralis* n. sp. (Ciliophora, Oxytrichidae). *J. Eukaryot. Microbiol.* 60, 455–466.
- Medlin, L., Elwood, H.J., Stickel, S., Sogin, M.L., 1988. The characterization of enzymatically amplified eukaryotic 16S-like rRNA-coding regions. *Gene* 71, 491–499.
- Miao, M., Shao, C., Chen, X., Song, W., 2011. Evolution of discocephalid ciliates: molecular, morphological and ontogenetic data support a sister group of discocephalids and pseudoamphisiellids (Protozoa, Ciliophora) with establishment of a new suborder Pseudoamphisiellina subord. n. *Sci. China Life Sci.* 54, 634–641.
- Nylander, J.A.A., 2004. MrModeltest, Version 2.0. Evolutionary Biology Centre, Uppsala University Press, Uppsala.
- Page, R.D.M., 1996. Tree view: an application to display phylogenetic trees on personal computers. *Comput. Appl. Biosci.* 12, 357–358.
- Ronquist, F., Huelsenbeck, J.P., 2003. MrBAYES 3: Bayesian phylogenetic inference under mixed models. *Bioinformatics* 19, 1572–1574.
- Shao, C., Song, W., Al-Rasheid, K.A.S., Berger, H., 2011. Redefinition and reassignment of the 18-cirri genera *Hemigastrostyla*, *Oxytricha*, *Urosomoida*, and *Actinotricha* (Ciliophora, Hypotrichida), and description of one new genus and two new species. *Acta Protozool.* 50, 263–287.
- Shao, C., Ding, Y., Al-Rasheid, K.A.S., Al-Farraj, A.S., Warren, A., Song, W., 2013a. Establishment of a new hypotrichous genus, *Heterotachysoma* n. gen. and notes on the morphogenesis of *Hemigastrostyla enigmatica* (Ciliophora, Hypotrichida). *Eur. J. Protistol.* 49, 93–105.
- Shao, C., Pan, X., Jiang, J., Ma, H., Al-Rasheid, K.A.S., Warren, A., Lin, X., 2013b. A redescription of the oxytrichid *Tetmemena pustulata* (Müller, 1786) Eigner, 1999 and notes on morphogenesis in the marine urostylid *Metaurostylopsis salina* Lei et al., 2005 (Ciliophora, Hypotrichida). *Eur. J. Protistol.* 49, 272–282.
- Shi, X., Warren, A., Song, W., 2002. Studies on the morphology and morphogenesis of *Allotricha curdsi* nov. spec. (Ciliophora, Hypotrichida). *Acta Protozool.* 41, 397–405.
- Singh, J., Kamra, K., 2013. *Paraurosomoida indiensis* gen. nov., sp. nov., an oxytrichid (Ciliophora, Hypotrichida) from Kyongnosla Alpine Sanctuary, including note on non-oxytrichid Dorso-marginalia. *Eur. J. Protistol.* 49, 600–610.
- Singh, J., Kamra, K., Sapra, G.R., 2013. Morphology, ontogenesis, and molecular phylogeny of an Indian population of *Cyrtohymena* (*Cyrtohymenides*) *shii*, including remarks on the subgenus. *Eur. J. Protistol.* 49, 283–297.
- Song, W., 1990. A comparative analysis of the morphology and morphogenesis of *Gonostomum strenua* (Engelmann, 1862) (Ciliophora, Hypotrichida) and related species. *J. Protozool.* 37, 249–257.
- Song, W., 2001. Morphology and morphogenesis of the marine ciliate *Ponturostyla enigmatica* (Dragesco & Dragesco-Kernéis, 1986) Jankowski, 1989 (Ciliophora, Hypotrichida, Oxytrichidae). *Eur. J. Protistol.* 37, 181–197.
- Song, W., Warren, A., 1999. Observations on morphogenesis in a marine ciliate *Tachysoma ovata* (Protozoa: Ciliophora: Hypotrichida). *J. Mar. Biol. Ass. U. K.* 79, 35–38.
- Song, W., Wilbert, N., 1997a. Morphological investigations on some free living ciliates (Protozoa, Ciliophora) from China seas with description of a new hypotrichous genus *Hemigastrostyla* nov. gen. *Arch. Protistenkd.* 148, 413–444.
- Song, W., Wilbert, N., 1997b. Morphological studies on some free living ciliates from marine biotopes in Qingdao, China, with descriptions of three new species: *Holosticha warreni* nov. spec., *Tachysoma ovata* nov. spec. and *T. dragescoi* nov. spec. *Eur. J. Protistol.* 33, 48–62.
- Song, W., Wilbert, N., 2002. Faunistic studies on marine ciliates from the Antarctic benthic area, including descriptions of one epizoic form, 6 new species and 2 new genera (Protozoa: Ciliophora). *Acta Protozool.* 41, 23–61.
- Stamatakis, A., Hoover, P., Rougemont, J., 2008. A rapid bootstrap algorithm for the RAxML Web servers. *Syst. Biol.* 57, 758–771.
- Tamura, K., Dudley, J., Nei, M., Kumar, S., 2007. MEGA4: molecular evolutionary genetics analysis (MEGA) software version 4.0. *Mol. Biol. Evol.* 24, 1596–1599.
- Wallengren, H., 1900. Zur Kenntnis der vergleichenden Morphologie der hypotrichen Infusorien. *Bih. K. Svensk. VetenskAkad. Handl.* 26, 1–31.
- Weisse, T., Moser, M., Scheffel, U., Stadler, P., Berendonk, T., Weithoff, G., Berger, H., 2013. Systematics and species-specific response to pH of *Oxytricha acidotolerans* sp. nov. and *Urosomoida* sp. (Ciliophora, Hypotrichida) from acid mining lakes. *Eur. J. Protistol.* 49, 255–271.
- Wilbert, N., 1975. Eine verbesserte Technik der Protargolimprägnation für Ciliaten. *Mikrokosmos* 64, 171–179.
- Yi, Z., Song, W., 2011. Evolution of the order Urostylida (Protozoa, Ciliophora): new hypotheses based on multi-gene information and identification of localized incongruence. *PLoS ONE* 6, e17471.
- Yi, Z., Katz, L.A., Song, W., 2012. Assessing whether alpha-tubulin sequences are suitable for phylogenetic reconstruction of Ciliophora with insights into its evolution in euplotids. *PLoS ONE* 7, e40635.